

Correlation Between Measured Mechanical and Microphysical Parameters for an Irradiated Pressure Vessel Material

W. B. Waeber, G. Solt, P. Tipping

Paul Scherrer Institute, Villigen PSI, Switzerland

F. Frisius

Research Centre GKSS, Geesthacht, FRG

O. M. Mercier

Paul Scherrer Institute, Villigen PSI, Switzerland

Abstract. Results of recent mechanical [1] and neutron scattering studies [2] have been combined in order to search for useful empirical correlations between radiation induced changes of mechanical and microphysical properties. The investigated RPV steel contained 0.17 wt% copper, it was irradiated in a test reactor to four different neutron fluences and subjected to various annealing schedules.

1. Introduction

Reasons for considering annealing procedures as applied to reactor pressure vessels have been given large space in the corresponding literature [3,4]. One of the aims of such programmes would be plant life extension. Along this line, work has also been carried out at PSI to obtain answers to the questions 'what effect would have various heat treatments on a typical medium Cu-content RPV steel', and 'would these effects be significant enough for the implementation of extended specific case studies in Switzerland' [5,6].

Investigations at PSI have been carried out along two lines: (i) by studying mechanical properties responding to irradiation and annealing [1,7,8] and (ii) by measuring the evolution with heat treatments of the microstructural parameters, such as the radius of irradiation induced precipitates [2,9,10]. The objective of this work is to combine the data resulting from these approaches, to study the trends in such empirical correlations, in order to possibly achieve a deeper understanding of steel embrittlement mechanisms.

In the following two sections the specific material investigated, irradiation and heat treatment procedures and the mechanical testing and neutron scattering results are summarized. In section 4 we discuss the correlation of defect size and density with Charpy parameters, and section 5 contains the conclusions.

2. Material, irradiation and heat treatments

In this section some relevant information on the material investigated, the specimens, irradiation conditions and annealing schedules will be given. Related investigations have been carried out in the frame of a programme which has been defined and discussed in refs. [5,6].

The type of RPV steel studied is a forging of 270 mm thickness, heat treated to 875°C in 7h, hold for 10h, water quenched, tempered to 635°C in 6h, hold for 11h, furnace cooled to 300°C and then air cooled. Alloy and impurity elements of interest in wt % are Si0.29, Mn1.47, Ni0.87, P0.02 and Cu0.17.

The standard loading of the irradiation capsule consisted of 30 Charpy, 18 precracked Charpy, 6 tensile specimens, two 3-point-bend-bars and a variable number of mini specimens to serve for various microphysical investigation techniques.

Irradiation conditions have been controlled by thermocouples and neutron monitors and were otherwise determined by several factors: (i) the position relative to the core, which together with the tailoring elements determined the overall neutron flux (125 x flux level of a typical PWR) and the neutron spectrum for $E > 1\text{MeV}$. (ii) The time at a given flux determined the fluence; the nominal values have been chosen to be 0.5, 1.7, 3.0 and $5.0 \times 10^{19}\text{cm}^{-2}$. (iii) The specific construction of the irradiation capsule which was part of a gas loop circulating a gas mixture of helium/nitrogen at normal pressure. Together with the reactor- γ -intensity heating up the steel specimens, this formed a device permitting to keep the specimen temperature at a level of 290°C , achieved by controlling the gas mixture. The temperature profile over the specimen height of 37cm has been achieved to stay within $\pm 5^{\circ}\text{C}$ in 80 % and $\pm 7^{\circ}\text{C}$ in 100 % of the irradiation time by choosing a specific gas gap geometry between the specimen holder and the capsule.

Heat treatments $A = 455^{\circ}\text{C}/168\text{h}$ and $A' = 455^{\circ}\text{C}/1.5\text{h}$ have been chosen after a detailed study of isothermal hardness recovery determinations [1]. With these schedules a number of individual specimens have been annealed in the hot cell. However, for purposes of obtaining full sets of specimens with IAR condition, i.e. after an intermediate A treatment (at half of the above mentioned fluence values) of the fully instrumented irradiation capsule in the hot cell, the capsule was reintroduced into the reactor for completion of the reirradiation (R) cycle (second half of the target fluence).

3. Mechanical testing, Neutron scattering

This section summarizes some of the results of systematic studies by means of impact testing on Charpy specimens [1,7] on the one hand and, essentially on the same specimen material, by means of small angle thermal neutron scattering [2,9] on the other hand.

Charpy specimens in the conditions U, UA, I, IA, IA' and IAR have been tested and the data have been analysed by using the usual $y = \tanh x$ function. Figure 1 shows the plots of the 41J-transition-temperature values vs fluence. The main conclusion that may be derived from this figure is the possibility of separating off an aging contribution from the recovery process, when considering the difference between the IA and IA' curves. For a detailed discussion of this point we refer to ref. [1]. However, a precise statement about embrittlement mechanisms cannot be drawn from such measurements. The only chance for reaching such objectives would be found in applications of microphysical techniques. In Table 1 are indicated the dosimetrically determined fluence values reached in the corresponding irradiation experiments as well as the measured temperature shifts $\Delta_{41J}T$ for the conditions I and IAR.

Small angle neutron scattering is a powerful mean to observe defects with well defined contours in the diameter range of 5 - 500 Å and to determine their density and size distribution, eventually giving information on composition and shape as well. In the present context voids, various point defect agglomerates and precipitating second phase particles may be produced as a result of fast neutron bombardment. These will appear at the origin of additional diffracted intensity as compared to the unirradiated, otherwise identical sample. For the present work the experimental facility [11] at the FRG-1 reactor in Geesthacht was used, the selection of 'cold' neutrons ($E < 5.2\text{meV}$) from the thermal neutron beam and the detectors measuring the elastically scattered intensity from the magnetized sample are the same as in refs. [2,9,10].

The physical-metallurgical information is summarized in the pair of scattering curves as shown in Figure 2. Such curves are obtained for each sample condition, showing the radiation induced scattering for two scattering geometries with respect to the direction of magnetization in the sample. If the inhomogeneities embedded in the field of homogeneous magnetization have the same size as the underlying spatial inhomogeneities, called 'particles', what should reasonably be the case for voids or non-magnetic precipitates as well, the two cross section curves in the figure are only shifted from each other, and the shift characterizes the particle composition. The size distribution of the particles can be deduced from the curves by a straightforward procedure [9], the accuracy of which improves with better statistics (more measuring time) and broader angular range ($\kappa = (4\pi/\lambda)\sin(\theta/2)$, where θ is the scattering angle). In Table 1 and in the following section we limit the discussion to the average particle radii \bar{R} and the total volume fractions f of the particles (volume of one particle times their

number density) for the various sample conditions. On the base of the measured shift of the curves the particles are identified as copper containing precipitates.

4. Correlations between Charpy shift, defect size and density

Empirical correlations may be useful for extrapolation purposes into domains where no measurements exist, or they may inspire further research and give useful indications (in this context) for modelling embrittlement mechanisms. However, it should be stated clearly that such correlations hold true only for the specific material under investigation.

In this sense Table 1 was used to plot in Figure 3 the average radius \bar{R} and the volume fraction f vs the Charpy shift $\Delta_{41J}T$ which is used here as a measure of the degree of embrittlement. By taking $x_I = \{\text{flux, fluence, spectrum, irradiation temperature}\}$ and $x_A = \{\text{annealing temperature, time}\}$ as independent variables, we may then describe in a phenomenological way, say, $\bar{R} = F_{mat}(x_I, x_A)$, $mat = \{\text{material dependent parameters}\}$. The Charpy shift is now described as the functional $\Delta T = G_{mat}(x_I, x_A, \bar{R})$. Depending on whether $x_A = 0$ or $x_A \neq 0$ we find, that

$$\Delta T_{(I)} = G_{mat}(x_I, 0, \bar{R}|_{x_A=0}) \quad \text{and} \quad \Delta T_{(IAR)} = G_{mat}(x_I, x_A, \bar{R}|_{x_A \neq 0})$$

represent two curves in the $f, \bar{R} - \Delta T$ plane (the projections along the x_I -axis of curves with $x_A = 0$ and with $x_A \neq 0$). In order to draw conclusions on the base of these curves, one has to be aware of the fact that 2 points on the curves having the same value $f = f_0$ do not belong to the same fluence, so that the corresponding 'samples' cannot be used as qualifiers for two different heat treatments related to the same irradiation dose. On the other hand, interrelation of the parameters may lead to useful observations; in the above example a measured value f_0 for an IAR specimen is much more 'serious', from the point of view of embrittlement, than the same f_0 measured for an I-specimen, since it implies a much larger ΔT .

There are some further observations which can be taken from Figure 3:

- There seems to be no (or only weak) correlation between ΔT and \bar{R} . Hence, measuring only \bar{R} in company with Charpy parameters would not be sufficient to predict the degree of embrittlement.
- In the case of the I-condition: for a fixed \bar{R} (which is more or less fulfilled in this case), low values of f , i.e. a low number density of defects, produces less embrittlement and vice versa. Such a monotonic, approximately linear correlation was to be expected for smaller doses. However, there is a transition to a saturation value (approximately the nominal Cu-content of the material investigated) where any correlation between ΔT and f seems to be lost: this substantiates the assumption that inhomogeneities causing embrittlement consist mainly of precipitating copper.
- In the case of the IAR-condition: at least in the domain of measurement there seems to exist a linear correlation $f - \Delta T$ which however differs from the I-condition. This correlation may, of course, also saturate for higher shift (fluence) values.
- For a given value of $\Delta_{41J}T$ (and constant \bar{R}) the number density of defect agglomerates in the I case is much higher than in the IAR case.

The question of how these observations have to be validated in the light of existing models of interaction between defect agglomerates and dislocations [12], may be answered via the correlation $f, \bar{R} - \sigma_y - \Delta T$ ($\sigma_y = \text{yield strength}$). The latter correlation $\sigma_y - \Delta T$ is linear [8], which together with the Russel-Brown theory $\bar{R} - \sigma_y$, indicates a qualitative agreement with the trends as found in Figure 3.

5. Conclusions

Unless for a given material a maximum set of correlations between all 'independent' parameters is being considered and worked out, it will be difficult to draw generally valid, material independent conclusions on embrittlement mechanisms. The attempt was made in this work to combine results of mechanical testing and of microphysical studies on a specific RPV steel. We note the following points:

- Such empirical correlations are important since they may indicate hints for modelling embrittlement mechanisms.
- There are microphysical parameters like the defect agglomerate radius \bar{R} which are at best only very weakly correlated with the Charpy transition temperature shift ΔT . Such parameters are nevertheless important to know since they do contribute to a fundamental understanding of radiation damage.
- There are other microphysical parameters, like the defect density, which correlate much stronger with macroscopic mechanical parameters. This is true also in conjunction with heat treatments on the irradiated material, however in somewhat weaker form.
- The accuracy of measured parameters has to be improved further, in order to come to more precise statements about this complex kind of correlations.
- A study of the formation and stability of the defects during irradiation, and a detailed study of the interaction of defect agglomerates with dislocations is needed, in order to understand what sizes, volume fractions, structures (coherent/incoherent precipitates) or chemical compositions of precipitates are the less or the most effective in causing embrittlement.

References

- [1] P. Tipping, W.B. Waeber and O. Mercier, Proc. NEA/CSNI - UNIPED Meeting on Life-limiting and Regulatory Aspects of Reactor Core Internals and Pressure Vessels, Swedish Nuclear Power Inspectorate 1988, 473-487.
- [2] G. Solt, F. Frisius, W.B. Waeber and W. Bühner, Proc. 14th Intern. Symp. on Effects of Radiation on Materials, June 27-29, 1988, Andover, Mass., ASTM, in press.
- [3] L.E. Steele, ed., "Radiation embrittlement and surveillance of nuclear reactor pressure vessels, An international study", ASTM STP 819, Philadelphia, 1983.
- [4] J.R. Hawthorne, "Survey of Post-Irradiation Heat Treatment as a Means to Mitigate Radiation Embrittlement of Reactor Vessel Steels", NUREG/CR-0486, NRL Report 8287, Naval Research Laboratory, Washington, D.C., Feb. 14 1979.
- [5] W.B. Waeber, D.H. Njo, in "Radiation Embrittlement of Nuclear Reactor Pressure Vessel Steels: An International Review" (Third Volume), L.E. Steele, ed., ASTM STP 1011, Philadelphia 1989, 48-69.
- [6] W.B. Waeber, G. Solt, U. Zimmerman, P. Tipping and B. Tirbonod, Proc. NEA/CSNI - UNIPED Meeting on Life-limiting and Regulatory Aspects of Reactor Core Internals and Pressure Vessels, Swedish Nuclear Power Inspectorate 1988, 421-442.
- [7] P. Tipping, W.B. Waeber and O. Mercier, in "Structural Mechanics in Reactor Technology", ed. by F.H. Wittmann, A.A. Balkema, Rotterdam/Boston 1987, vol G, 115-127.
- [8] P. Tipping, W.B. Waeber, this conference.
- [9] G. Solt, F. Frisius and W.B. Waeber, In "Radiation Embrittlement of Nuclear Reactor Pressure Vessel Steels: An International Review" (Third Volume), ed. by L.E. Steele, ASTM STP 1011, Philadelphia 1989, 229-242.
- [10] G. Solt, U. Zimmermann, W.B. Waeber, O. Mercier, F. Frisius and K. Ghazi-Wakili, in "Structural Mechanics in Reactor Technology", ed. by F.H. Wittmann, A.A. Balkema, Rotterdam 1987, vol. G, p.105-113.
- [11] F. Frisius and M. Naraghi, Atomkernenergie 29, 139, 1977
- [12] K.C. Russel, L.M. Brown, Acta Metallurgica, vol.20, 1972, 969-974.

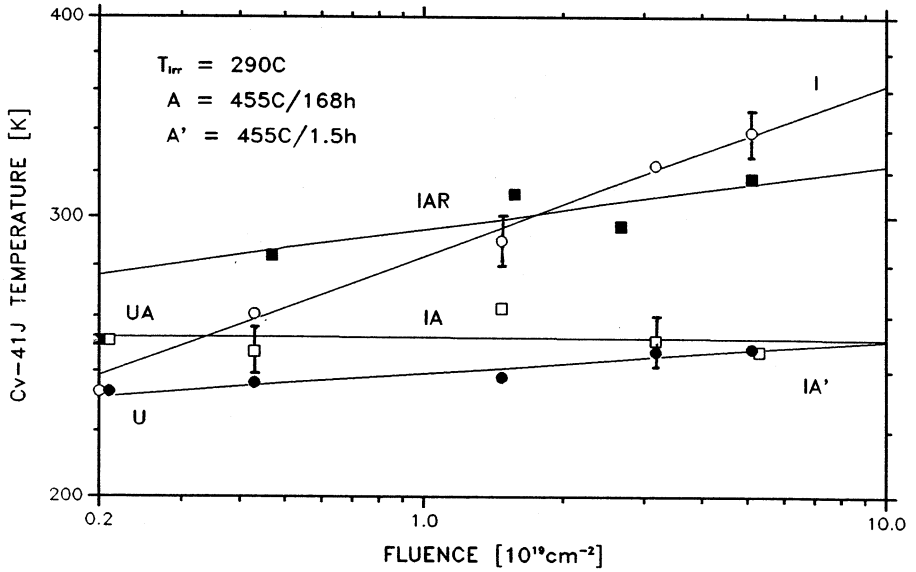


Figure 1. Together with the IAR-condition, the data for the 41J-transition temperature in the IA-condition are plotted as a function of fluence and similarly for the I- and IA'-conditions. Since, for the material considered, the IA'-curve lies below the IA-curve for low and intermediate fluence values, a separation between aging and recovery processes has been possible [1]. The shift values in Table 1 are obtained from the data in this figure by subtracting the value 233°K of the U-condition.

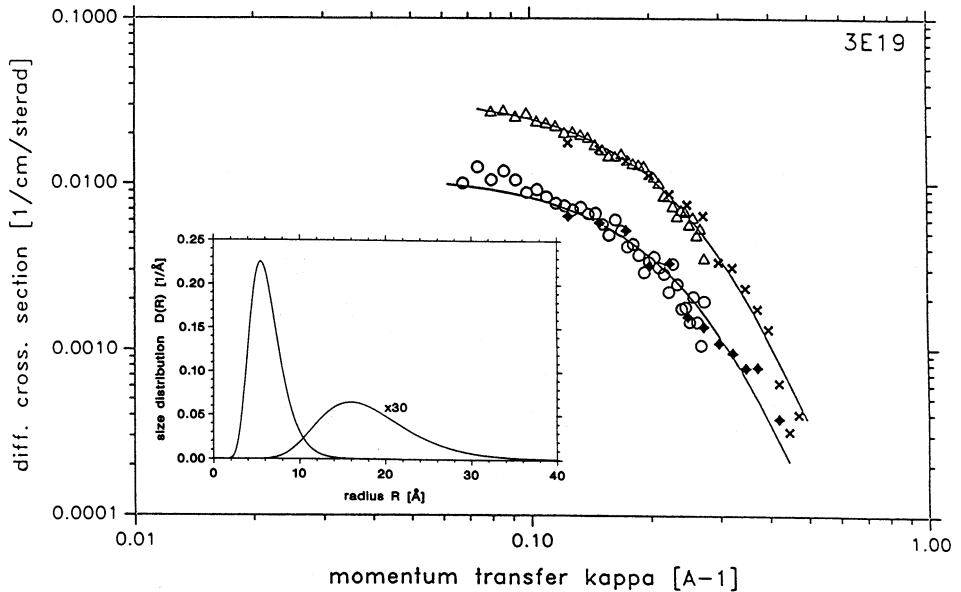


Figure 2. Macroscopic cross section of the irradiation defects in the steel for a fluence of $5.1 \times 10^{19} \text{ cm}^{-2}$ [2]. The larger values measured for $\vec{\kappa} \perp \vec{M}$ (triangles: SANS and x: DENS) represent the sum of nuclear and magnetic scattering contributions, the lower points (o: SANS and full squares: DENS) show the nuclear cross section alone, as measured for $\vec{\kappa} \parallel \vec{M}$. The theoretical fit (solid lines) to these curves gives a mean radius $\bar{R} = 8.9 \pm 0.5 \text{\AA}$ for the spherically shaped radiation induced precipitates, present in a density of $1.34 \times 10^{18} / \text{cm}^3$. **Insert:** Size distribution of precipitates with intermediate annealing; the bimodal distribution leads to two mean radii ($\bar{R}_1 = 6.9 \text{\AA}$, $\bar{R}_2 = 20.0 \text{\AA}$). The 'large particle' component is multiplied by 30, for convenience.

Table 1. Fluence values, Charpy temperature shift, radius and volume fraction of Cu-containing precipitates [2], of the irradiated steel as described in section 2. The top line indicates the target fluences in the I- and IAR-conditions, 1st 4 columns and last 4 columns respectively.

	0.5	1.7	3.0	5.0	0.5	1.7	3.0	5.0
dosimetric fluence ($\pm\Delta, cm^{-2}$)	0.43	1.47	3.18	5.10	0.47	1.57	2.67	5.10
$\Delta_{41J}T$ ($\pm\Delta_T, ^\circ C$)	28	57	90	106	51	77	63	84
\bar{R} ($\pm\Delta_R, \text{\AA}$)	5.95	7.2	8.7	8.9	5.64	9.3	8.9	6.9
f ($\pm\Delta_f, \%$)	0.06	0.16	0.18	0.16	0.04	0.06	0.05	0.092

$$\Delta \sim 10 \%, \quad \Delta_T \sim 5, \quad \Delta_R^I \sim 1.0, \quad \Delta_R^{IAR} \sim 2.0, \quad \Delta_f \sim 0.01.$$

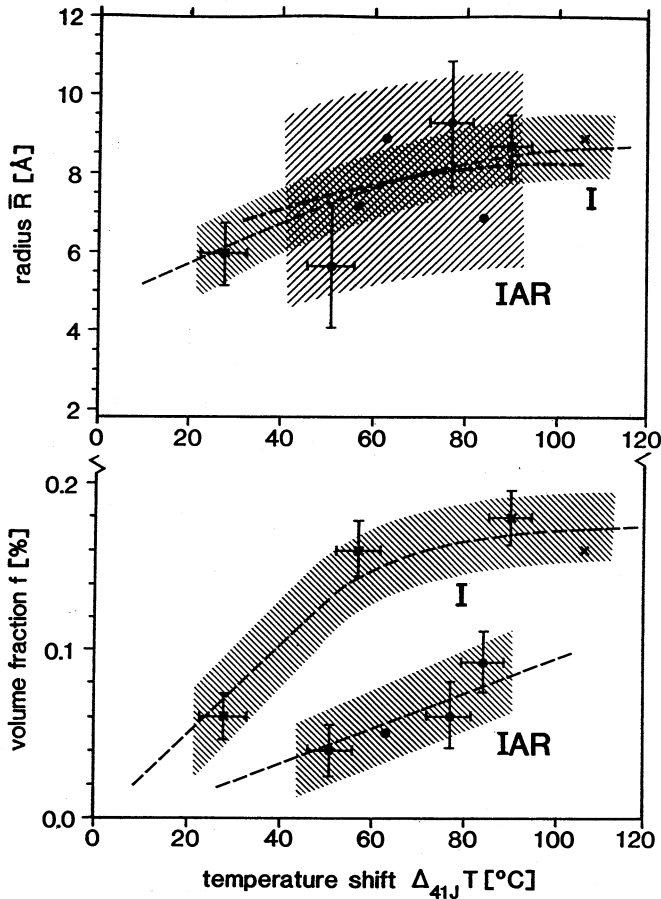


Figure 3. Empirical correlations between the ductile to brittle transition temperature shift ΔT and the average particle radius \bar{R} (upper part) and the volume fraction f (lower part) respectively. For clarity reasons not all experimental error bars are plotted. The pairs of hatched bands correspond to the as irradiated (I) and irradiated-annealed-reirradiated (IAR, see text) conditions.

Authors' Index

AHMAD J. 105
ANDERSON N. 13, 57
BAGCHI G. 39, 69
BARTHELET B. 117
CHANG T.Y. 69
CHANG T.-Y. 13
CHEN J.T. 69
CHEVANNE H. 117
CHEVERTON R.D. 131
CHOKSHI N.C. 39, 57, 69
CLAUSS D.B. 33
CONOSCENTE J.P. 99
COSTELLO J.F. 87, 93
CURRERI J. 93
DEVITA V. 81
DEWALL K.G. 7
EDER S.J. 99
FRISIUS F. 149
GUZY D.J. 45, 75
HAGGAG F.M. 143
HARRIS S.P. 99

HELIOT J. 117
HOFMAYER C.H. 93
HSIEH B.J. 87
ISKANDER S.K. 143
JENG D.C. 69
JULIEN J.T. 33
KATO W.Y. 93
KAWAKAMI S. 93
KELLY G. 69
KENNEALLY R.M. 45, 69
KOBAYASHI T. 19
KONNO T. 19
KOT C.A. 87
KRAMER G.S. 105
KURTZ R.J. 123
MARSCHALL C.W. 105
MERCIER O.M. 149
MOHAMMADIOUN B. 65
MURPHY A.J. 45, 65, 69
MURRAY R.C. 51

MUSCARA J. 123
NANSTAD R.K. 131, 143
NARUSE Y. 19
PARK Y.J. 93
PARKS M.B. 25, 33
PENNEL W.E. 131
PETERS S.W. 33
PHILIPPACOPOULOS A.J. 39
REITER L. 69
ROBINSON G.C. 131
SATOU T. 19
SHAUKAT S.K. 39, 57
SOLT G. 149
SRINIVASAN M.G. 87
STEELE JR R. 1
SUMODOBILA B.N. 99
TANG H.T. 93
TIPPING P. 149
WAEBER W.B. 149
WILKOWSKI G.M. 105

